

Article

Friction Welding of Polycarbonate Plate and Aluminum Foam Fabricated by Precursor Foaming Process

Yoshihiko Hangai ^{1,*}, Yuta Yamamoto ¹, Yu Goto ¹, Kenji Okada ¹  and Nobuhiro Yoshikawa ²¹ Graduate School of Science and Technology, Gunma University, Kiryu 376-8515, Japan² Institute of Industrial Science, The University of Tokyo, Tokyo 153-8505, Japan

* Correspondence: hanhan@gunma-u.ac.jp

Abstract: Aluminum foam is expected to be one of the candidates for lightweight materials for structural components as it is lightweight and has excellent shock absorption and sound absorption properties. However, aluminum foam has low tensile and flexural strength due to its thin cell walls. Therefore, aluminum foam is used by combining with dense materials. In particular, with the recent trend toward multi-materials, research on the combination with lightweight resins is expected. In this study, we attempted to join aluminum foam fabricated by the precursor method to a thermoplastic resin polycarbonate (PCTA) plate by friction welding. It was found that the aluminum foam and PCTA plate can be joined in about 1 min by friction welding, by rotating the aluminum foam at 2000 rpm and pressing 1 mm into the PCTA plate. In addition, in the friction welding of aluminum foam and PCTA plate, it was found that the pores of the aluminum foam were maintained without being collapsed. The anchoring effect is presumably caused by the penetration of PCTA softened by the frictional heat generated by the friction welding into the pores. Furthermore, tensile tests of the joined samples showed that fracture occurred either at the joining interface or at the base material of the aluminum foam, and that the joining strength was equivalent to the tensile strength of the aluminum foam itself.

Keywords: cellular materials; dissimilar joining; foam; resin; polymer–metal joints; solid-state welding



Citation: Hangai, Y.; Yamamoto, Y.; Goto, Y.; Okada, K.; Yoshikawa, N. Friction Welding of Polycarbonate Plate and Aluminum Foam Fabricated by Precursor Foaming Process. *Metals* **2023**, *13*, 1366. <https://doi.org/10.3390/met13081366>

Academic Editor: Thomas Fiedler

Received: 10 July 2023

Revised: 25 July 2023

Accepted: 28 July 2023

Published: 29 July 2023



Copyright: © 2023 by the authors. Licensee MDPI, Basel, Switzerland. This article is an open access article distributed under the terms and conditions of the Creative Commons Attribution (CC BY) license (<https://creativecommons.org/licenses/by/4.0/>).

1. Introduction

Aluminum foam is expected to be one of the candidates for lightweight materials for structural components as it is lightweight and has excellent shock absorption and sound absorption properties [1–4]. However, aluminum foam has low tensile and flexural strength due to its thin cell walls. Therefore, aluminum foam is used by combining with dense materials, such as sandwich panels [4–8]. In particular, with the recent trend toward multi-materials [9–13], research on the combination with lightweight resins is expected.

Generally, aluminum foam and dense materials are combined using adhesives. However, the use of general adhesives has problems with the spreading method and curing time. Therefore, composites without using the adhesives have also been attempted. Kitazono et al. [14] and Yuan et al. [15] applied liquid polyester resin and epoxy resin directly to the pores on the surface of aluminum foam and solidified it to fabricate composites. Matsumoto et al. [16] placed solid polyamide resin into the pores of the surface of the aluminum foam and filled the pores by melting the polyamide resin with a selective laser. Ilinzeer et al. [17] fabricated the sandwich structure by simultaneously fabricating carbon fiber-reinforced plastic plates as the surface material and allowing the matrix resin to penetrate the pores of the aluminum foam. Matsumoto et al. [18] attempted a friction stir incremental forming process for joining polymethyl methacrylate plate and nickel foam. Fujioka et al. [19] applied hot-pressing to join polycarbonate plates and aluminum foam. Kim et al. [20] and Iwata et al. [21] fabricated a porous structure using additive manufacturing and other methods to join polyamide-6 and carbon fiber-reinforced thermoplastic plates, and then

hot-pressed to join them together. However, hot-pressing requires heating of the aluminum foam, which poses problems of heating time and energy. Because there are few studies on direct bonding, there is a need for an easier and more productive joining method. Hangai et al. have attempted to join porous aluminum fabricated by the sintering and dissolution process (SDP) [22–26] to polycarbonate (PCTA) and acrylic resin plates by friction welding [27–29]. Friction welding [30,31] is a simple and productive joining method, which is one of the solid-state welding methods [32–35], allowing strong joining without melting the material. The porous aluminum is rotated at a high rotating rate and pressed against the PCTA plate to soften the PCTA by frictional heat, which allows the PCTA to penetrate the pores, joining them by the anchor effect. Joining can be completed in about one minute, making it easy and highly productive. Tensile tests of joined samples between porous aluminum with 70% and 80% porosity and resin plates have shown that joining strength comparable to the tensile strength of porous aluminum can be achieved.

In this study, we attempted to join aluminum foam made by the precursor method [36–38], which is a practical method for fabricating aluminum foam, to a PCTA plate by friction welding. Porous aluminum fabricated by SDP has small pores, each of which is connected to the others. In contrast, the pores in aluminum foam are large and independent; that is, the pore structures differ significantly from those of the porous aluminum fabricated by SDP. We examined whether friction welding could be performed without pore fracture and whether aluminum foam with large pores and independent pores could be joined to the PCTA plate, by observing the joined samples with X-ray CT and performing tensile tests to evaluate the joining strength.

2. Materials and Methods

2.1. Aluminum Foam Fabrication Method

Aluminum foam samples were fabricated by the precursor method utilizing friction stir welding (FSW) [39–44]. First, two Al-Si-Cu ADC12 alloy die-casting plates (210 mm × 80 mm × 3 mm) were prepared. FSW was performed with 1 wt.% of foaming agent powder (TiH₂, particle size less than 45 μm) and 5 wt.% of pore morphology stabilizer powder (Al₂O₃, particle size about 1 μm) between two ADC12 plates. For details, please refer to the literature [40,43]. Briefly, the tool was traversed at a tool rotating rate of 1200 rpm, a tool traversing speed of 120 mm/min, and a tilt angle of 3 degrees to mix and disperse the foaming agent powder and pore morphology stabilizer powder into the ADC12 plates. Precursors of 15 mm × 15 mm × 6 mm were taken from ADC12 plates after FSW and foamed in ambient air by optical heating using halogen lamps [45,46]. To obtain a shape suitable for friction welding, the aluminum foam was pressed immediately after foaming to prepare a flat aluminum foam (10 mm in thickness). The foamed aluminum can be formed into a flat shape without fracturing pores by pressing immediately after foaming before the temperature of the foamed aluminum drops below the liquidus temperature [47–49]. The surface of the pressed aluminum foam was milled to remove 1.2 mm–1.6 mm to expose the pores because the pressed aluminum foam had a dense skin layer on the surface.

2.2. Joining Methods

Figure 1 shows a schematic diagram of the joining method. First, as shown in Figure 1a, a rod made of SUS304 stainless steel with a diameter of 16 mm and a length of 100 mm was attached with an adhesive to the surface with a skin layer on the opposite side of the milled aluminum foam. Next, the attached SUS rod was fixed to the chuck of the milling machine. A plate of polycarbonate (PCTA), a thermoplastic resin, 60 mm × 50 mm and 8 mm thick, was used as the resin to be joined to the aluminum foam. The PCTA plate was fixed to the milling machine with tape. The aluminum foam rotated at 2000 rpm was pressed on the PCTA plate from above, as shown in Figure 1b. Pressing was performed manually. First, once the aluminum foam and PCTA plate were in contact, the foamed aluminum was slowly pressed into the PCTA plate by 1 mm, and then the rotation was

stopped to cool the sample. The pressing time t was about 50 s to 80 s. Seven trials were performed. Additionally, to measure the temperature during joining, one trial was also performed at 2000 rpm and one trial at 370 rpm. A video camera (Sony Corporation, Tokyo, Japan) was used to record the joining process. The exact pressing time was estimated after the joining was completed by reviewing the video camera images since the pressing was performed manually.

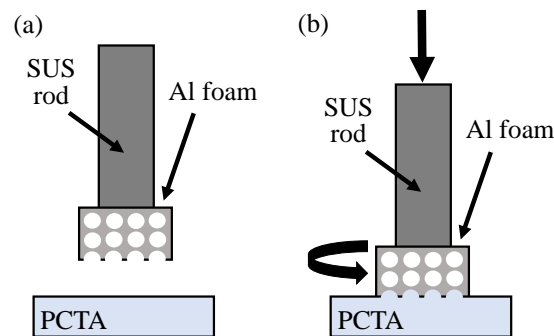


Figure 1. Friction welding of aluminum foam to PCTA plate. (a) Initial state. (b) During friction welding.

2.3. X-ray CT Imaging Method

X-ray CT imaging of the joined samples was performed to observe whether the pores in the aluminum foam were not fractured and whether PCTA had penetrated the pores. The X-ray tube voltage and current were 80 kV and 30 μ A, respectively, and cone-beam CT was employed. The pixel equivalent length was 75–80 μ m/pixel.

2.4. Tensile Test Methods

The joined samples were subjected to tensile test to evaluate the strength of them. Tensile tests were performed using an Instron 5582 (Instron, Kawasaki, Japan). Figure 2 shows a schematic diagram of the tensile test. The SUS rod used for joining was attached to the chuck at the top of the tensile testing machine. The PCTA plate was hooked to a jig made of Al-Mg-Si alloy A6061, and a similar SUS rod attached to the bottom of the jig was attached to the chuck at the bottom of the tensile testing machine for the tensile test. Tensile stress was determined by dividing the tensile load obtained from the testing machine by the area of aluminum foam on the joining surface obtained from X-ray CT images. The tensile stress at fracture was defined as the joining strength σ_t .

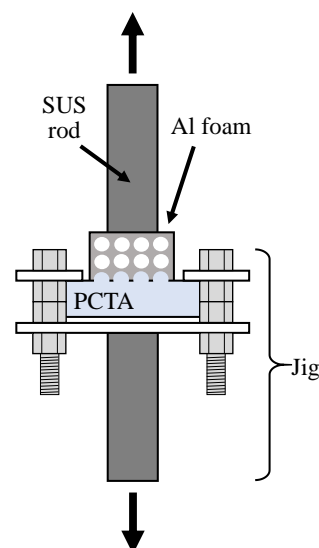


Figure 2. Tensile test of sample joined with aluminum foam and PCTA plate.

Cross-section of the fracture surface after tensile test was observed using a digital microscope (KEYENCE Corporation, Osaka, Japan).

3. Results and Discussion

3.1. Joining Test Results

Figure 3 shows the foaming precursor and pressing process. First, the precursor was placed under the halogen lamp on the right side, as shown in Figure 3a, and then heated and foamed as shown in Figure 3b. The precursor foamed spherically when foamed. Once the precursor was foamed, it was moved to the bottom of the pressing equipment on the left side for pressing as shown in Figure 3c. Figure 3d shows the aluminum foam after pressing. The foam was formed into a flat shape without fracture.

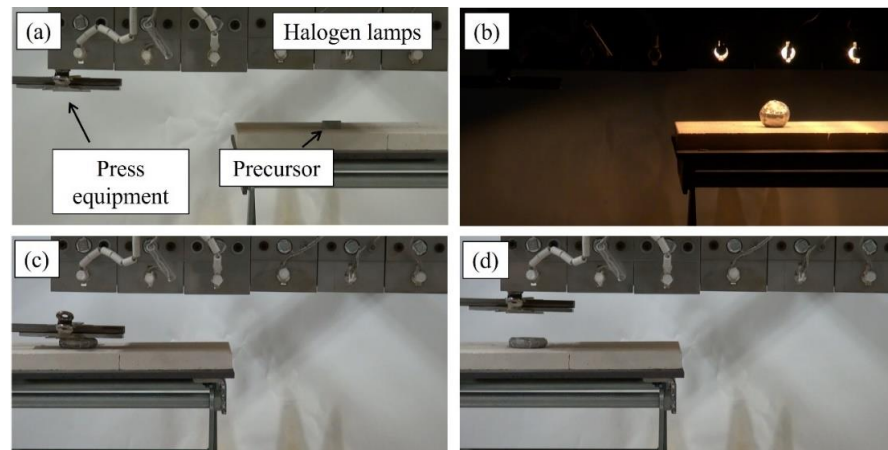


Figure 3. Foaming precursor and pressing process. (a) Initial state before heating and foaming precursor. (b) Foamed precursor. (c) Press forming of foamed aluminum. (d) Press-formed aluminum foam.

Figure 4 shows the joining of aluminum foam to a PCTA plate. Figure 4a shows the initial state before joining. It was rotated and pressed into the PCTA plate. At the beginning of pressing, the PCTA plate was scraped by aluminum foam as shown in Figure 4b, and a small amount of cutting chips was observed. After a short time, the PCTA softened due to the frictional heat between the aluminum foam and the PCTA plate, and burrs were generated as shown in Figure 4c. At this time, the softened PCTA is expected to penetrate the pores. After 1 mm was pressed in, the rotation was stopped as shown in Figure 4d. After cooling, the joined sample was unfixed from the chuck of the milling machine to remove. During removal, the aluminum foam and PCTA plate remained unseparated.

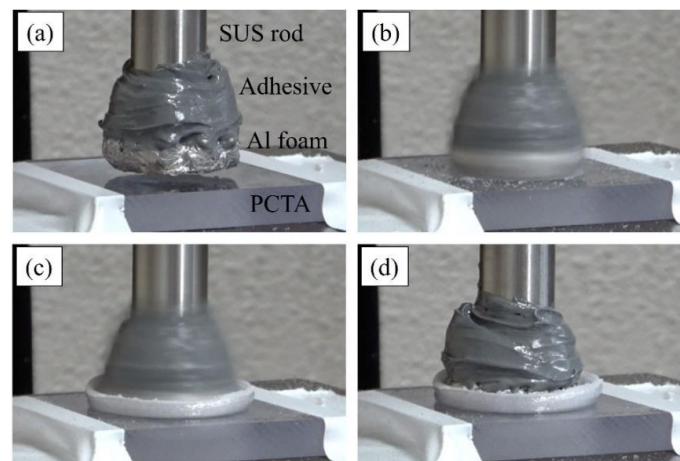


Figure 4. Friction welding of aluminum foam to PCTA plate at 2000 rpm. (a) Initial state before joining. (b) Beginning of joining. (c) During joining. (d) After joining.

Figure 5 shows the joining of aluminum foam to a PCTA plate at 370 rpm, a slower rotating rate, for comparison. Figure 5a shows the beginning of pressing, corresponding to Figure 4b when pressing at 2000 rpm. As in the case of 2000 rpm, the PCTA plate was scraped by the aluminum foam and cutting chips were generated. Figure 5b shows the sample immediately after the rotation was stopped after pressing in 1 mm. At 370 rpm, the PCTA was not softened, and the PCTA plate was scraped by the aluminum foam and only cutting chips were scattered around it. No joining was achieved, and the aluminum foam and the PCTA plate were separated when removed from the milling machine.

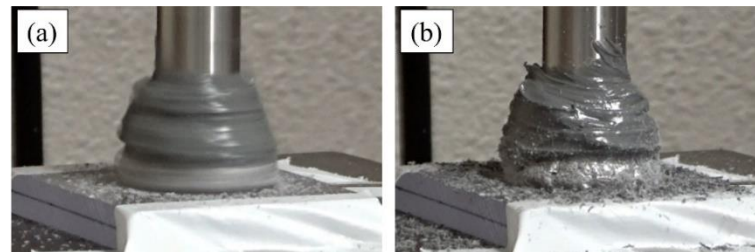


Figure 5. Friction welding of aluminum foam to PCTA plate at 370 rpm. (a) Beginning of joining. (b) After joining.

Figure 6 shows the temperature T of the PCTA plate during joining, as measured by a thermocouple. The results are also shown for a tool rotating rate of 370 rpm. As shown in Figure 7, the measurement was performed at the center of the SUS rod, 1 mm below the surface of the aluminum foam at the final pressing. As shown by the dotted lines in Figure 6, the glass transition temperature of PCTA is 150 °C (catalog value [50]), which is well above the glass transition temperature at 2000 rpm. Consequently, PCTA was sufficiently softened and the softened PCTA penetrated into the pores, and joining was achieved. In contrast, at 370 rpm, PCTA only reached the vicinity of the glass transition temperature, indicating that PCTA did not soften sufficiently. As a result, only cutting chips were generated and no joining was achieved. Note that the solidus temperature of ADC12 alloy is 515 °C [51]; therefore, the friction welding applied in this study did not reach the temperature at which ADC12 alloy softens.

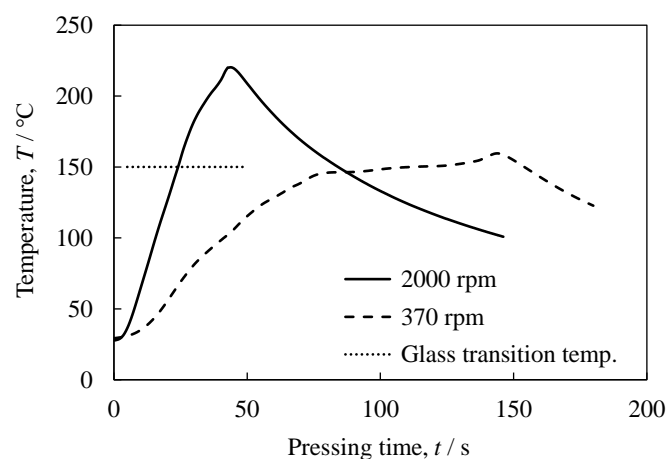


Figure 6. Temperature T of the PCTA plate during joining.

Figure 8 shows a typical example of a sample joined at a rotating rate of 2000 rpm and a pressing time of 62 s. Figure 8a shows the joined sample viewed from the side. Although the aluminum foam was not visible due to the burr of the PCTA, it was joined without separation when removed from the milling machine. Figure 8b shows the joining sample viewed from the back of PCTA. Aluminum foam is not visible, but it was observed that PCTA has been stirred and whitened. Figure 8c is an X-ray CT image of the joined sample

viewed from the side, with the internal cross-section observed from the direction shown in Figure 8a. The upper part is aluminum foam and the lower part is a PCTA plate. In the aluminum foam, the white areas are aluminum and the black areas are pores. The bright white area above the aluminum foam is part of a bonded SUS rod. PCTA is shown in gray, the intermediate color between aluminum and pore. PCTA penetrates the pores of aluminum foam as indicated by white arrows near the boundary between the aluminum foam and PCTA plate. Figure 8d is an X-ray CT image near the interface between the aluminum foam and PCTA plate, showing the internal cross-section from the direction of Figure 8b. As in Figure 8c, many pores where PCTA penetrated were observed as indicated by the white arrows, indicating that an anchoring effect was expected to exhibit. Also, if the pores collapse, the surface pores are closed by the collapsed cell walls, but no such pores are observed. The pores were maintained without collapsing by friction welding, and PCTA penetrated those pores.

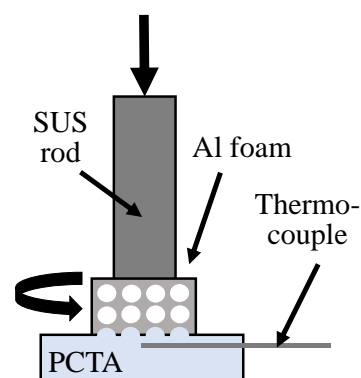


Figure 7. Temperature measurement method during joining.

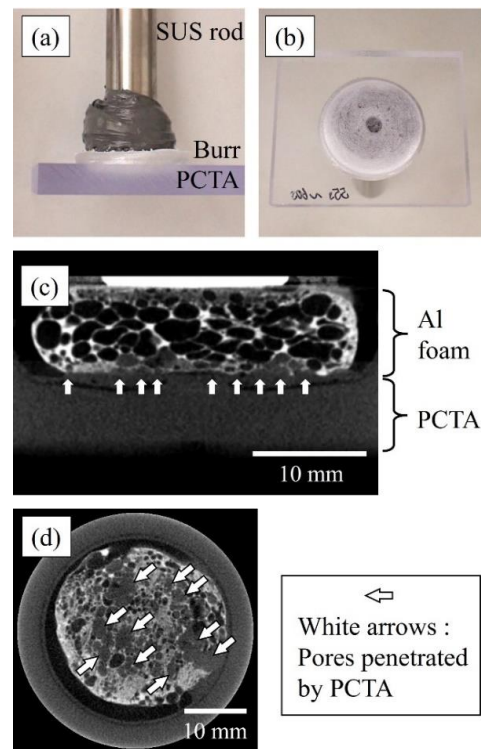


Figure 8. Sample joined at a rotating rate of 2000 rpm and a pressing time of 62 s. (a) Sample viewed from the side. (b) Sample viewed from the back of PCTA plate. (c) X-ray CT image of sample viewed from the side. (d) X-ray CT image of sample near the interface between the aluminum foam and PCTA plate.

3.2. Tensile Test Results of Joining Samples

Figure 9a–c show the joined sample shown in Figure 8 during the tensile test, and Figure 9d shows its load-displacement curve. (a)–(c) in Figure 9d correspond to the images during the tensile test shown in Figure 9a–c. The load increased linearly with increasing displacement, leading directly to fracture. The fracture was observed in the vicinity of the joined interface. Similar trends were observed for the other six joined samples and the one sample joined for temperature measurements. In the preliminary experiments of this study, the PCTA plate was 3 mm thick, not the 8 mm thick plate used in this study.

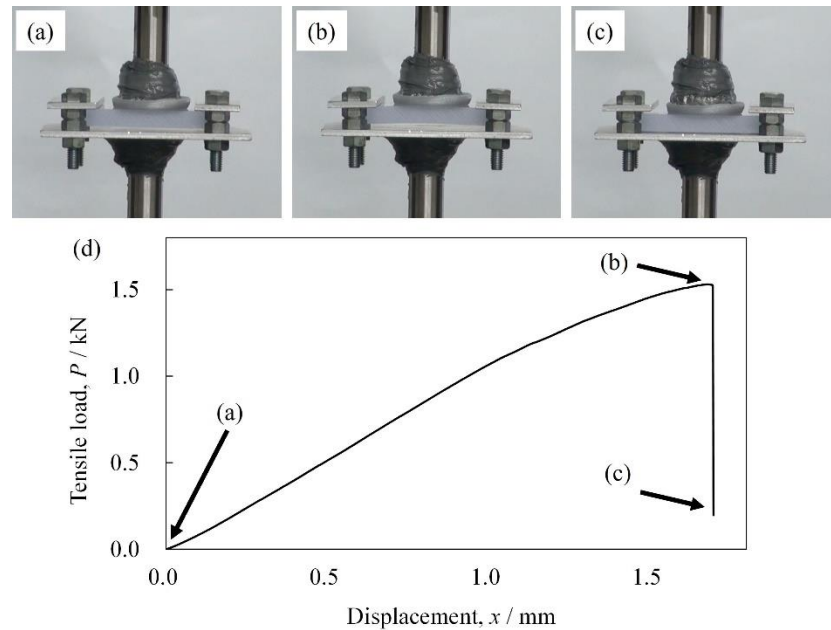


Figure 9. Joined sample during tensile test. (a) Initial state before tensile test. (b) Immediately before fracture. (c) After fracture. (d) Load-displacement curve during tensile test.

However, as shown in Figure 10 during the tensile test of a sample joined to a 3 mm-thick PCTA plate, the PCTA plate deflected significantly during the tensile test, and the strength of the joined sample could not be accurately measured. Therefore, PCTA plates with a thickness of 8 mm were used to avoid as much deflection during the tensile test as possible. However, a thin PCTA plate with a thickness of 3 mm can be joined by friction welding in the same way as in the case of a PCTA plate with a thickness of 8 mm, indicating that friction welding can be applied regardless of the thickness of the PCTA plate.

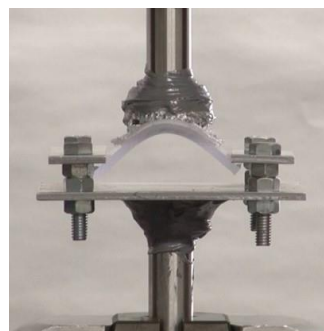


Figure 10. Tensile test of a sample joined to a 3 mm thick PCTA plate.

Figure 11 shows the fracture surface after the tensile test of a sample shown in Figure 8 joined at a rotating rate of 2000 rpm and a pressing time of 62 s. Figure 11a shows the

fracture surface of the aluminum foam side and Figure 11b shows the fracture surface of the PCTA side. The fracture occurred near the joining interface, but the fracture surface on the aluminum foam side was uneven, unlike the flat surface before joining. On the fracture surface on the PCTA side, a part of aluminum foam was observed, and PCTA was observed in its pores as indicated by the black arrows. It is assumed that PCTA penetrated the pores, reinforcing the aluminum foam near the joining interface and exhibiting an anchoring effect, resulting in fracture at the pore locations where PCTA did not penetrate. In the fracture surface on the PCTA side, where no aluminum foam is observed, the surface of the PCTA has unevenness that transfers the pore shape of the aluminum foam. This is due to the softened PCTA penetrating the pores by friction welding and being pulled out during the tensile test.

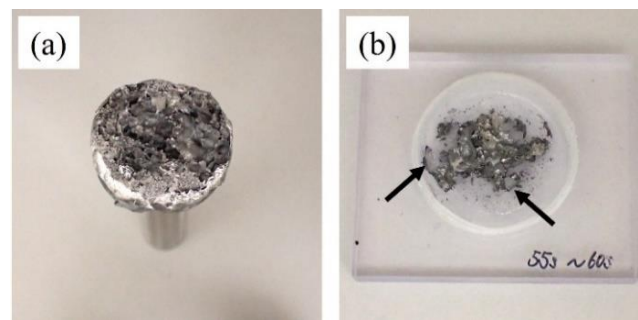


Figure 11. Fracture surface after tensile test of a sample joined at a rotating rate of 2000 rpm and a pressing time of 62 s. (a) Aluminum foam side. (b) PCTA side.

Figure 12 shows a digital microscope observation of the interface between the aluminum foam and PCTA at the cross-section of the fracture surface on the PCTA side shown in Figure 11b. The lower part is PCTA and the upper part is the aluminum foam remaining on the PCTA side of the fracture surface. The first layer of pores is filled with PCTA, and PCTA is observed filling the interior of the pores and tightly attached to the cell walls as shown by black arrows. Similar results were observed in other areas. Note that bubbles were observed in a part of PCTA, which were probably generated by the vaporization of PCTA due to frictional heat. Therefore, it is necessary to consider temperature control in future studies.

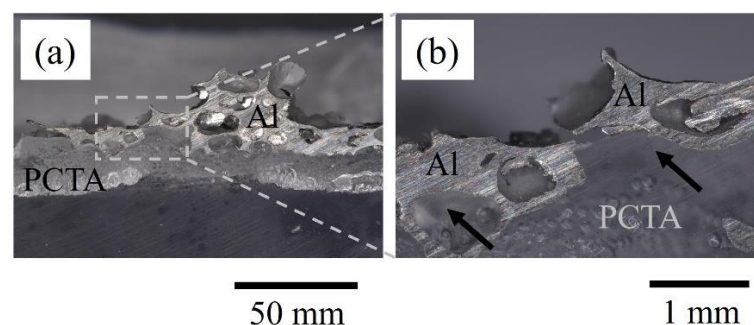


Figure 12. (a) Digital microscope image of a cross-section of Figure 11b. (b) Enlarged image of (a).

Figure 13 shows the relationship between joining strength σ_t and indentation time t . A sample joined for temperature measurement ($t = 53$ s) was also included. Five tensile tests were also conducted on the aluminum foam itself, and the minimum and average tensile strengths are also shown as dotted lines. The tensile strength of aluminum foam is significantly affected by the internal pore structures. Especially since the aluminum foam in this study is formed thinly, the variation is noticeable. The tensile strength of the aluminum foam in this study ranged from 1.36 MPa to 4.64 MPa, with an average value of 2.74 MPa. This indicates that the joined samples in this study have a joining strength comparable

to the tensile strength of foamed aluminum. Namely, it was shown that friction welding can join aluminum foam and PCTA plate with a pressing time of about one minute and that joining strength equivalent to the tensile strength of the aluminum foam itself can be obtained.

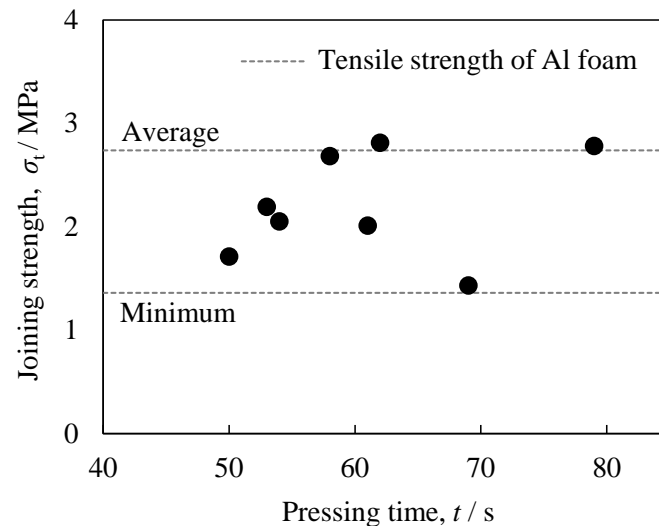


Figure 13. Relationship between joining strength σ_t and indentation time t .

In this study, since the pressing was performed manually, the pressing time was estimated after the joining was completed by reviewing the video camera images. To obtain an exact relationship between indentation time and joining strength, it is necessary to automate the indentation operation to achieve accurate indentation time and constant indentation speed, which is a future research topic. Note that at the joining time $t = 69$ s and, although the joining strength is higher than the minimum tensile strength of the aluminum foam, it is slightly lower than that of the other samples. The fracture surfaces are shown in Figure 14a,b. The fracture surface on the PCTA side had little aluminum foam on it, indicating that fracture at the interface was dominant. Figure 14c shows an X-ray CT image in the vicinity of the joining interface. Compared to the joined sample exhibiting high joining strength shown in Figure 8d, there are fewer pores where the PCTA penetrated. Although it remains to be clarified why the amount of PCTA penetration is sometimes high and sometimes low, it is considered to be related to the porosity, pore size, and pore arrangement in the vicinity of the joining interface. However, it was found that if PCTA can penetrate the pores, the anchoring effect allows the joining strength to be as high as that of the aluminum foam itself.

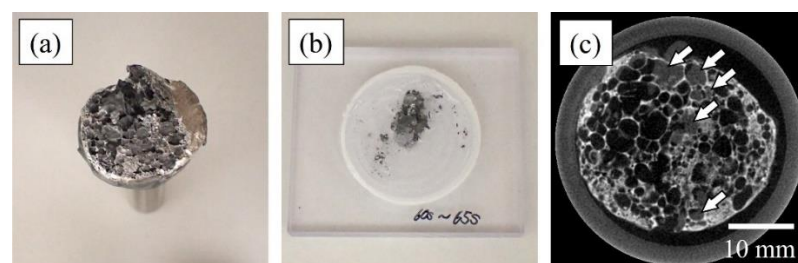


Figure 14. Fracture surface after tensile test and X-ray CT image of a sample joined at a rotating rate of 2000 rpm and a pressing time of 69 s. (a) Aluminum foam side. (b) PCTA side. (c) X-ray CT image of a sample near the interface between the aluminum foam and PCTA plate.

4. Conclusions

In this study, we attempted to join aluminum foam fabricated by the precursor method to a thermoplastic resin PCTA plate by friction welding. The results obtained are shown below.

- (1) By rotating the aluminum foam at 2000 rpm and pressing 1 mm into the PCTA plate, it was found that the aluminum foam and PCTA plate can be joined in about 1 min by friction welding.
- (2) In the friction welding of aluminum foam and PCTA plate, it was found that the pores of the aluminum foam were maintained without being collapsed. The anchoring effect is presumably caused by the penetration of PCTA softened by the frictional heat generated by the friction welding into the pores.
- (3) Tensile tests of the joined samples showed that fracture occurred either at the joining interface or at the base material of the aluminum foam and that the joining strength was equivalent to the tensile strength of the aluminum foam itself.

Author Contributions: Conceptualization, Y.H.; investigation, Y.Y., Y.G., K.O. and N.Y.; writing—original draft preparation, Y.H. and Y.Y.; writing—review and editing, Y.H. All authors have read and agreed to the published version of the manuscript.

Funding: This research was funded by the JST-Mirai Program, grant number JPMJMI19E5, Japan.

Data Availability Statement: Not applicable.

Acknowledgments: This work was partly performed under the Cooperative Research Program of the Institute for Joining and Welding Research Institute, Osaka University. The authors would like to thank Takaaki Suzuki of Gunma University for his help with digital microscope observation.

Conflicts of Interest: The authors declare no conflict of interest.

References

1. Banhart, J. Light-Metal Foams—History of Innovation and Technological Challenges. *Adv. Eng. Mater.* **2013**, *15*, 82–111. [[CrossRef](#)]
2. García-Moreno, F. Commercial Applications of Metal Foams: Their Properties and Production. *Materials* **2016**, *9*, 85. [[CrossRef](#)]
3. Wan, T.; Liu, Y.; Zhou, C.; Chen, X.; Li, Y. Fabrication, properties, and applications of open-cell aluminum foams: A review. *J. Mater. Sci. Technol.* **2021**, *62*, 11–24. [[CrossRef](#)]
4. Ji, C.; Huang, H.; Wang, T.; Huang, Q. Recent advances and future trends in processing methods and characterization technologies of aluminum foam composite structures: A review. *J. Manuf. Processes* **2023**, *93*, 116–152. [[CrossRef](#)]
5. Banhart, J.; Seeliger, H.W. Aluminium Foam Sandwich Panels: Manufacture, Metallurgy and Applications. *Adv. Eng. Mater.* **2008**, *10*, 793–802. [[CrossRef](#)]
6. Banhart, J.; Seeliger, H.W. Recent Trends in Aluminum Foam Sandwich Technology. *Adv. Eng. Mater.* **2012**, *14*, 1082–1087. [[CrossRef](#)]
7. Hangai, Y.; Kamada, H.; Utsunomiya, T.; Kitahara, S.; Kuwazuru, O.; Yoshikawa, N. Aluminum alloy foam core sandwich panels fabricated from die casting aluminum alloy by friction stir welding route. *J. Mater. Process. Technol.* **2014**, *214*, 1928–1934. [[CrossRef](#)]
8. Zhang, J.; An, Y.; Ma, H. Research Progress in the Preparation of Aluminum Foam Composite Structures. *Metals* **2022**, *12*, 2047.
9. Lambiase, F.; Balle, F.; Blaga, L.A.; Liu, F.C.; Amancio, S.T. Friction-based processes for hybrid multi-material joining. *Compos. Struct.* **2021**, *266*, 113828. [[CrossRef](#)]
10. Hirose, A. Dissimilar joining for multi-materials structures. *J. Japan Inst. Light Met.* **2021**, *71*, 188–196. [[CrossRef](#)]
11. Nandhakumar, R.; Venkatesan, K. A process parameters review on selective laser melting-based additive manufacturing of single and multi-material: Microstructure, physical properties, tribological, and surface roughness. *Mater. Today Commun.* **2023**, *35*, 105538. [[CrossRef](#)]
12. Nazir, A.; Gokcekaya, O.; Billah, K.M.M.; Ertugrul, O.; Jiang, J.C.; Sun, J.Y.; Hussain, S. Multi-material additive manufacturing: A systematic review of design, properties, applications, challenges, and 3D printing of materials and cellular metamaterials. *Mater. Des.* **2023**, *226*, 111661. [[CrossRef](#)]
13. Ostolaza, M.; Arrizubieta, J.I.; Lamikiz, A.; Plaza, S.; Ortega, N. Latest Developments to Manufacture Metal Matrix Composites and Functionally Graded Materials through AM: A State-of-the-Art Review. *Materials* **2023**, *16*, 1746. [[CrossRef](#)] [[PubMed](#)]
14. Kitazono, K.; Suzuki, R.; Inui, Y. Novel strengthening method of closed-cell aluminum foams through surface treatment by resin. *J. Mater. Process. Technol.* **2009**, *209*, 3550–3554. [[CrossRef](#)]
15. Yuan, J.Y.; Chen, X.; Zhou, W.W.; Li, Y.X. Study on quasi-static compressive properties of aluminum foam-epoxy resin composite structures. *Compos. Part B-Eng.* **2015**, *79*, 301–310. [[CrossRef](#)]

16. Matsumoto, R.; Kanatani, S.; Utsunomiya, H. Filling of surface pores of aluminum foam with polyamide by selective laser melting for improvement in mechanical properties. *J. Mater. Process. Technol.* **2016**, *237*, 402–408. [[CrossRef](#)]
17. Ilinzeer, S.; Rupp, P.; Weidenmann, K.A. Influence of corrosion on the mechanical properties of hybrid sandwich structures with CFRP face sheets and aluminum foam core. *Compos. Struct.* **2018**, *202*, 142–150. [[CrossRef](#)]
18. Matsumoto, R.; Sakaguchi, H.; Otsu, M.; Utsunomiya, H. Plastic joining of open-cell nickel foam and polymethyl methacrylate (PMMA) sheet by friction stir incremental forming. *J. Mater. Process. Technol.* **2020**, *282*, 116691. [[CrossRef](#)]
19. Fujioka, T.; Hangai, Y.; Mitsugi, H.; Amagai, K. Press Bonding of Heated Porous Aluminum and Polycarbonate. *J. Japan Inst. Met. Mater.* **2022**, *86*, 17–21. [[CrossRef](#)]
20. Kim, S.-G.; Suzuki, A.; Takata, N.; Kobashi, M. Effect of hot-press thermal history on joint strength of A5052/Polyamide-6 hybrid structure via a porous layer. *J. Mater. Process. Technol.* **2020**, *276*, 116388. [[CrossRef](#)]
21. Iwata, K.; Suzuki, A.; Kim, S.-G.; Takata, N.; Kobashi, M. Enhancing the solid-state joinability of A5052 and CFRTP via an additively manufactured micro-structure. *J. Mater. Process. Technol.* **2022**, *306*, 117629. [[CrossRef](#)]
22. Zhao, Y.Y.; Sun, D.X. A novel sintering-dissolution process for manufacturing Al foams. *Scr. Mater.* **2001**, *44*, 105–110. [[CrossRef](#)]
23. Hakamada, M.; Kuromura, T.; Chino, Y.; Yamada, Y.; Chen, Y.; Kusuda, H.; Mabuchi, M. Monotonic and cyclic compressive properties of porous aluminum fabricated by spacer method. *Mater. Sci. Eng. A-Struct. Mater. Prop. Microstruct. Process.* **2007**, *459*, 286–293. [[CrossRef](#)]
24. Stanev, L.; Kolev, M.; Drenchev, B.; Drenchev, L. Open-Cell Metallic Porous Materials Obtained Through Space Holders-Part I: Production Methods. A Review. *J. Manuf. Sci. Eng.-Trans. ASME* **2017**, *139*, 050801. [[CrossRef](#)]
25. Stanev, L.; Kolev, M.; Drenchev, B.; Drenchev, L. Open-Cell Metallic Porous Materials Obtained Through Space Holders-Part II: Structure and Properties. A Review. *J. Manuf. Sci. Eng.-Trans. ASME* **2017**, *139*, 050802. [[CrossRef](#)]
26. Atwater, M.A.; Guevara, L.N.; Darling, K.A.; Tschopp, M.A. Solid State Porous Metal Production: A Review of the Capabilities, Characteristics, and Challenges. *Adv. Eng. Mater.* **2018**, *20*, 1700766. [[CrossRef](#)]
27. Hangai, Y.; Kishimoto, R.; Ando, M.; Mitsugi, H.; Goto, Y.; Kamakoshi, Y.; Suzuki, R.; Matsubara, M.; Aoki, Y.; Fujii, H. Friction welding of porous aluminum and polycarbonate plate. *Mater. Lett.* **2021**, *304*, 130610. [[CrossRef](#)]
28. Hangai, Y.; Omika, K.; Inoue, M.; Kitamura, A.; Mitsugi, H.; Fujii, H.; Kamakoshi, Y. Effect of porosity of aluminum foam on welding between aluminum foam and polycarbonate plate during friction welding. *Int. J. Adv. Manuf. Technol.* **2022**, *120*, 1071–1078. [[CrossRef](#)]
29. Matsushima, Y.; Hangai, Y.; Mitsugi, H.; Fujii, H. Effects of Rotational Speed and Processing Time on Bonding Strength of Porous Aluminum and Thermoplastic Resin during Friction Welding. *J. Japan Inst. Met. Mater.* **2022**, *86*, 71–76. [[CrossRef](#)]
30. Uday, M.B.; Fauzi, M.N.A.; Zuhailawati, H.; Ismail, A.B. Advances in friction welding process: A review. *Sci. Technol. Weld. Join.* **2010**, *15*, 534–558. [[CrossRef](#)]
31. Li, W.Y.; Vairis, A.; Preuss, M.; Ma, T.J. Linear and rotary friction welding review. *Int. Mater. Rev.* **2016**, *61*, 71–100. [[CrossRef](#)]
32. Rathee, S.; Maheshwari, S.; Siddiquee, A.N.; Srivastava, M. A Review of Recent Progress in Solid State Fabrication of Composites and Functionally Graded Systems Via Friction Stir Processing. *Crit. Rev. Solid State Mater. Sci.* **2018**, *43*, 334–366. [[CrossRef](#)]
33. Cai, W.; Daehn, G.; Vivek, A.; Li, J.J.; Khan, H.; Mishra, R.S.; Komarasamy, M. A State-of-the-Art Review on Solid-State Metal Joining. *J. Manuf. Sci. Eng.-Trans. ASME* **2019**, *141*, 031012. [[CrossRef](#)]
34. Meng, X.; Huang, Y.; Cao, J.; Shen, J.; dos Santos, J.F. Recent progress on control strategies for inherent issues in friction stir welding. *Prog. Mater. Sci.* **2021**, *115*, 100706. [[CrossRef](#)]
35. Skowrońska, B.; Bober, M.; Kołodziejczak, P.; Baranowski, M.; Kozłowski, M.; Chmielewski, T. Solid-State Rotary Friction-Welded Tungsten and Mild Steel Joints. *Appl. Sci.* **2022**, *12*, 9034.
36. Baumgartner, F.; Duarte, I.; Banhart, J. Industrialization of powder compact foaming process. *Adv. Eng. Mater.* **2000**, *2*, 168–174.
37. Duarte, I.; Vesenjak, M.; Vide, M.J. Automated Continuous Production Line of Parts Made of Metallic Foams. *Metals* **2019**, *9*, 531. [[CrossRef](#)]
38. Parveez, B.; Jamal, N.A.; Anuar, H.; Ahmad, Y.; Aabid, A.; Baig, M. Microstructure and Mechanical Properties of Metal Foams Fabricated via Melt Foaming and Powder Metallurgy Technique: A Review. *Materials* **2022**, *15*, 5302. [[PubMed](#)]
39. Hangai, Y.; Utsunomiya, T.; Hasegawa, M. Effect of tool rotating rate on foaming properties of porous aluminum fabricated by using friction stir processing. *J. Mater. Process. Technol.* **2010**, *210*, 288–292. [[CrossRef](#)]
40. Hangai, Y.; Takahashi, K.; Yamaguchi, R.; Utsunomiya, T.; Kitahara, S.; Kuwazuru, O.; Yoshikawa, N. Nondestructive observation of pore structure deformation behavior of functionally graded aluminum foam by X-ray computed tomography. *Mater. Sci. Eng. A-Struct. Mater. Prop. Microstruct. Process.* **2012**, *556*, 678–684.
41. Papantoniou, I.G.; Kyriakopoulou, H.P.; Pantelis, D.I.; Manolacos, D.E. Fabrication of MWCNT-reinforced Al composite local foams using friction stir processing route. *Int. J. Adv. Manuf. Technol.* **2018**, *97*, 675–686. [[CrossRef](#)]
42. Shandley, R.; Maheshwari, S.; Siddiquee, A.N.; Mohammed, S.; Chen, D.L. Foaming of friction stir processed Al/MgCO₃ precursor via flame heating. *Mater. Res. Express* **2020**, *7*, 026515. [[CrossRef](#)]
43. Hangai, Y.; Morohashi, H.; Aoki, Y.; Mitsugi, H.; Fujii, H. Process of simultaneously fabricating and foaming precursor using frictional heat generated during friction stir welding. *Int. J. Adv. Manuf. Technol.* **2022**, *121*, 3207–3214. [[CrossRef](#)]
44. Abidi, M.H.; Moiduddin, K.; Siddiquee, A.N.; Mian, S.H.; Mohammed, M.K. Development of Aluminium Metal Foams via Friction Stir Processing by Utilizing MgCO₃ Precursor. *Coatings* **2023**, *13*, 162.

45. Hangai, Y.; Amagai, K.; Omachi, K.; Tsurumi, N.; Utsunomiya, T.; Yoshikawa, N. Forming of aluminum foam using steel mesh as die during foaming of precursor by optical heating. *Opt. Laser Technol.* **2018**, *108*, 496–501. [[CrossRef](#)]
46. Hangai, Y.; Nagahiro, R.; Ohashi, M.; Amagai, K.; Utsunomiya, T.; Yoshikawa, N. Shaping of aluminum foam during foaming of precursor using steel mesh with various opening ratios. *Metals* **2019**, *9*, 223. [[CrossRef](#)]
47. Hangai, Y.; Ohashi, M.; Nagahiro, R.; Amagai, K.; Utsunomiya, T.; Yoshikawa, N. Press forming of aluminum foam during foaming of precursor. *Mater. Trans.* **2019**, *60*, 2464–2469. [[CrossRef](#)]
48. Hangai, Y.; Kawato, D.; Ando, M.; Ohashi, M.; Morisada, Y.; Ogura, T.; Fujii, H.; Nagahiro, R.; Amagai, K.; Utsunomiya, T.; et al. Nondestructive observation of pores during press forming of aluminum foam by X-ray radiography. *Mater. Charact.* **2020**, *170*, 110631. [[CrossRef](#)]
49. Hangai, Y.; Kawato, D.; Ohashi, M.; Ando, M.; Ogura, T.; Morisada, Y.; Fujii, H.; Kamakoshi, Y.; Mitsugi, H.; Amagai, K. X-ray Radiography Inspection of Pores of Thin Aluminum Foam during Press Forming Immediately after Foaming. *Metals* **2021**, *11*, 1226. [[CrossRef](#)]
50. MISUMI Group Inc. Technical Information. Available online: https://jp.misumi-ec.com/tech-info/categories/plastic_mold_design/pl09/c0840.html (accessed on 27 June 2023).
51. The-Japan-Institute-of-Light-Metals. *Structures and Properties of Aluminum*; The Japan Institute of Light Metals: Tokyo, Japan, 1991.

Disclaimer/Publisher’s Note: The statements, opinions and data contained in all publications are solely those of the individual author(s) and contributor(s) and not of MDPI and/or the editor(s). MDPI and/or the editor(s) disclaim responsibility for any injury to people or property resulting from any ideas, methods, instructions or products referred to in the content.